

Skipping motion of the surface scattering of ion beams

Y. H. Ohtsuki and K. Koyama

Department of Physics, Waseda University, Ohkubo, Shinjuku-ku, Tokyo, Japan

Y. Yamamura

Department of Applied Physics, Okayama College of Science, Ridaicho, Okayama, Japan

(Received 15 January 1979; revised manuscript received 23 April 1979)

We propose a new motion of the ion near the surface of a solid due to the surface potential of the dynamical polarization of the valence-electron cloud induced by the moving ion itself. Under some appropriate conditions the outgoing ions are forced to be drawn once again to the surface by this potential and go through with skipping motions. Computer simulation shows that a large number of ions are trapped in the skipping motions.

I. INTRODUCTION

In recent years, there has been a growing interest in ion scattering at the surface of a solid and ion emissions from the surface of a solid. Surface channeling and sputtering are two examples of these topics.¹ Many authors have been involved in developing analytical theories and computer simulations.

However, no authors took into account the potential due to the polarization of the electron cloud by the ion motion near the surface. It is obvious that the effect is negligible when the ions are scattered or emitted at a large angle to the surface, except in the very-low-energy cases. On the other hand, the force due to the surface potential will be very important for the ion motion at a small angle to the surface.

Here we show that the potential is effective under some conditions, by making use of general results on the surface potential obtained in a previous paper.² Next, in Sec. II, we propose conditions for the skipping motion of ions at the surface. In Sec. III we perform a computer simulation for the skipping motions.

II. SURFACE POTENTIAL AT THE SURFACE

The potential due to the dynamical polarization of the valence-electron cloud is derived by

$$\psi(1) = \int W(12) \rho^{\text{ext}}(2) d(2) \quad (1)$$

where (1) means the position vector \vec{r}_1 and time t_1 ,

$$\begin{aligned} \psi_S(\vec{r}_1, t_1) = & -\frac{1}{2} Z_1 e \int_0^\infty dk \frac{(\omega_S/v)^2}{k^2 + (\omega_S/v)^2} [J_0(k\rho_\pm) \exp(-k|vt_1 \pm \xi_\mp|) \Theta(-t_1) \\ & + J_0(k\rho_\pm) \exp(-k|vt_1 \mp \xi_\pm|) \Theta(t_1)] \quad (6) \end{aligned}$$

In the above the ion velocity vector \vec{v} is assumed to be $\vec{v} = (0, v \sin\theta, v \cos\theta)$, θ being the angle between the ion

and $\rho^{\text{ext}}(2)$ is the ion charge density imbedded in the valence-electron cloud:

$$\rho^{\text{ext}}(\vec{r}_2, t_2) = \delta(\vec{r}_2 - \vec{v}t_2) \quad (2)$$

The dynamical screened interaction $W(12)$ is calculated² at the surface by the many-body-problem technique, considering the diagram shown in Fig. 1.

In the previous paper² we have calculated the potential $\psi(1)$ which is very complicated, but expressed it in analytical manner. The potential $\psi(1)$ is divided into two parts, corresponding to the bulk- and the surface-plasmon contributions

$$\psi(1) = \psi_B(1) + \psi_S(1) \quad (3)$$

Each potential is represented by three terms as

$$\psi_S(1) = \psi_S^{\text{scr}}(1) + \psi_S^{\text{wake}}(1) + \psi_S^{\text{pol}}(1) \quad (4)$$

and

$$\psi_B(1) = \psi_B^{\text{scr}}(1) + \psi_B^{\text{wake}}(1) + \psi_B^{\text{pol}}(1) \quad (5)$$

In the above "scr" means the screening-field potential due to plasmon excitation and "wake" is the wake potential, "pol" indicates the polarization-wave potential.

In particular, the screening potential due to the surface-plasmon excitation, ψ_S^{scr} , plays an important role in the ion motion at the surface. The potential for the ion is given by²

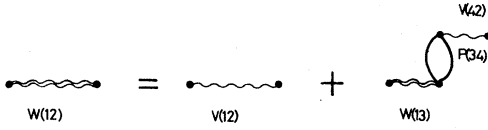


FIG. 1. Diagram for calculating the dynamical screened interaction $W(12)$. The bare Coulomb interaction and the polarization amplitude are denoted as $V(12)$ and $P(34)$, respectively. Detailed discussion about the calculation of $W(12)$ is given in Ref. 2.

direction and the z axis which is normal to the surface. ω_S is the surface-plasmon frequency. We also defined

$$\begin{aligned}\xi_{\pm} &= z \cos \theta \pm y \sin \theta, \\ \rho_{\pm}^2 &= x^2 + \eta_{\pm}^2, \\ \eta_{\pm} &= \mp z \sin \theta + y \cos \theta.\end{aligned}\quad (7)$$

When we consider a very small distance from the surface, so that $\omega_S t_1 < 1$, we obtain the potential for the ions,

$$\begin{aligned}\psi_S(t_1) &\simeq -\frac{\pi(Z_1 e)^2 \omega_S}{4\nu} \\ &\times \left[1 - \frac{4}{\pi} \alpha^2 \omega_S t_1 \ln(2\omega_S t_1 \alpha^2) - \frac{\omega_S t_1}{\pi} \right],\end{aligned}\quad (6')$$

where α is the small exit angle between the ion-beam direction and the surface, i.e., $\alpha = \frac{1}{2}\pi - \theta$.

In Fig. 2 we show an example of the potential for 30-keV protons scattered at a Ni surface as a function of $z = t_1 \nu \cos \theta$, for $\theta = 1^\circ$. We note that the potential barrier appearing at the surface is very large (order of 10 eV) and the ions are forced to be drawn to the surface.

Here we estimate the deviation angle due to the surface force by this potential. It is not so difficult to show the order of magnitude of $\psi_S(t_1)$ given by Eq.(6')

$$\psi_S(t_1) \simeq \frac{\pi(Z_1 e)^2 \omega_S}{4\nu}.\quad (8)$$

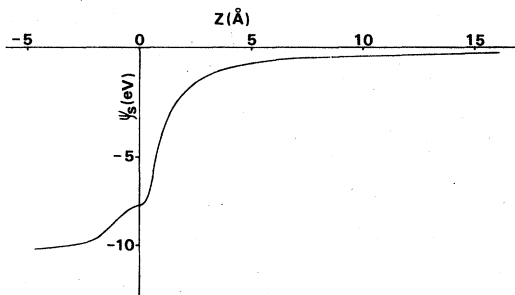


FIG. 2. Surface potential ψ_S for 30-keV protons scattered at a Ni surface as a function of $z = \nu(\cos \theta)t_1$, for $\theta = 1^\circ$.

So, the deviation angle $\Delta\alpha$ of ions moving away from the surface with energy E and at a small angle α to the surface is given by

$$E \Delta\alpha^2 = \frac{\pi(Z_1 e)^2 \omega_S}{4\nu}\quad (9)$$

or

$$\Delta\alpha = \frac{1}{2} Z_1 e \left(\frac{\pi \omega_S}{\nu E} \right)^{1/2}.\quad (10)$$

If $\Delta\alpha$ is larger than α , the ions scattered or emitted from the surface with the angle α to the surface are forced to be drawn once again to the surface. Then we could find ions which move with the skipping motion of a stone thrown onto a water surface.

If we take $E = 100$ keV, $Z_1 = 1$, and $\hbar\omega_p = \sqrt{2}\hbar\omega_S = 15$ eV, we obtain the deviation angle $\Delta\alpha = 0.4^\circ$. So, there is the possibility that the ions scattered or emitted from the surface at an angle smaller than 0.4° move with a skipping motion. In what follows we check the skipping motion by computer simulation.

III. COMPUTER SIMULATION OF THE EFFECT OF THE SURFACE POTENTIAL

In Sec. II we have discussed theoretically the possibility of skipping motions of scattered ions. It is very difficult to estimate analytically the effect of the surface force on surface scattering at a grazing angle and the characteristics of the motions.

In this section we employ a computer simulation, which is one of the most powerful techniques in studying surface scattering. In the present simulation a hydrogen beam of 30-keV energy is incident onto the (100) face of a Ni single crystal. The incidence planes are parallel to the $\langle 110 \rangle$ direction of the (100) surface or the $\langle 100 \rangle$ direction of the (100) surface. In the ensuing figures these incidence planes will be denoted by using the symbols $\langle 110 \rangle$ and $\langle 100 \rangle$, respectively.

A. Computation model

The simulation model was described in detail in Ref. 3; here we emphasize those aspects which are relevant to the interpretation of the present results or are added for the simulation of the skipping motions.

The present program describes the scattering process as a sequence of binary collisions and deals with all collision sets in a strictly sequential manner. The interatomic potential used for the binary collisions is a screened potential with the screening function given by the Molière approximation⁴ for the Thomas-Fermi function where we adopt the Firsov formula⁵ as a Thomas-Fermi screening length.

The scattering angle in the barycentric system and the time integral are given as

$$\theta = \pi - 2p \int_R^\infty dr [r^2 f(r)]^{-1},$$

$$\tau = (R^2 - p^2)^{-1/2} - \int_R^\infty dr \{ [f(r)]^{-1} - (1 - p^2/r^2)^{-1/2} \},$$

where

$$f(r) = [1 - p^2/r^2 - V(r)/E_r]^{1/2}.$$

In the above p is the impact parameter, E_r is the relative kinetic energy, $V(r)$ is the interatomic-force potential, and R is the apsis of the collision which is defined by $f(R) = 0$. Letting $z = a/r$ (a is the screening length) in the above equations and adopting the Everhart method⁶ in calculating the barycentric scattering angle, the scattering integrals are numerically evaluated by the four-point Gauss-Legendre quadrature at each collision event.

The present model includes thermal vibrations of target atoms. The anisotropy of the surface thermal vibration is also taken into account. We use the values $\Theta_D = \Theta_{D||} = 160$ K and $\Theta_{D\perp} = 110$ K,⁷ where $\Theta_{D\perp}$ and $\Theta_{D||}$ are the Debye temperatures related to displacements perpendicular and parallel to the surface, respectively, and Θ_D is that for the vibration of atoms in the bulk.

The neutralization effect plays a significant role in investigating the skipping motions, because this phenomenon will be observed only for a very small angle of incidence.

Since the standard Hagstrum formula⁸ for the neutralization probability overestimates for small distances s from the surface, we employ the following formula developed by Horiguchi *et al.*⁹:

$$P(s) = C \{ \exp(-2\kappa s) + (Bs + A) \exp[-(\kappa + a_0^{-1})s] + (Ds^2 + Es + F) \exp(-2a_0^{-1}s) \}, \quad (11)$$

where a_0 is the Bohr radius and A , B , C , D , E , F , and κ are proper constants depending on the target. This gives the neutralization probability P_e for an ion path,

$$P_e = \exp \left[- \int_{\text{path}} P(s) \frac{dt}{ds} ds \right]. \quad (12)$$

Since the mass ratio of the present collision partners is very large, the nuclear stopping power is negligible and the energy loss along the ion trajectory is mainly due to the inelastic collisions. The present program estimates the inelastic energy loss by the Firsov theory.¹⁰ Since this theory is not satisfactory for light ions, we modify the formula in the following manner¹¹:

$$Q(E, p) = c_1 k \sqrt{E} / (1 + c_2 p)^5, \quad (13)$$

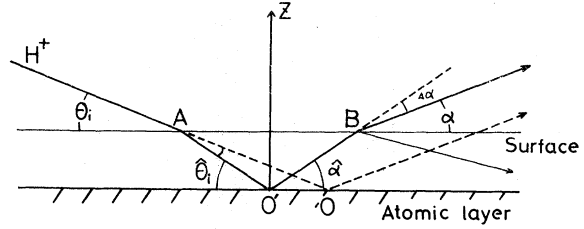


FIG. 3. Scheme of the ion trajectories near the surface — with surface force of step type, $\psi_s(0)$. - - - without surface force

where

$$\begin{aligned} c_1 &= 0.0594 (Z_1 + Z_2)^{5/3} / \sqrt{M_1} eV^{1/2}, \\ c_2 &= 0.304 (Z_1 + Z_2)^{1/3} \text{ \AA}^{-1}. \end{aligned} \quad (14)$$

Z_1 and Z_2 are the atomic numbers of the projectile and the target atom, respectively, M_1 is the atomic mass of the projectile, and k is an adjustment parameter. The value of k is determined by comparing the Northcliffe and Schilling data for the stopping power.¹¹

This is the first attempt to incorporate the surface force into the surface scattering. Under the circumstance that there are some ambiguities in determining the parameters in the formulas for the inelastic energy loss, the interatomic potential, and the thermal vibration of the surface atoms, and that we do not take into account the electron loss or capture process in the solid, it is difficult to estimate quantitatively the effects of the present force, because surface scattering at a grazing angle is very sensitive to the surface model employed in the simulation.

In the present simulation, we adopted the surface force derived from the potential $\psi_s(r_1, t_1)$, and the surface position at $z = L_s = \frac{1}{2} L_0$, L_0 being the lattice constant, which implies that the electron density is zero for $z > L_s$.

Figure 3 shows a scheme of the ion trajectories near the surface assuming the step-type function $\psi_s(0)$ as a surface potential given by Eq. (8) at $z = L_s$, where θ_i and α are the grazing and ejection angles, respectively. In the region $z < L_s$, we denote these angles by $\hat{\theta}_i$ and $\hat{\alpha}$, respectively.

The present model will underestimate the neutralization escape probability outside the surface and overestimate its probability inside the surface, if the neutralization process is determined only by the Auger neutralization.

B. Simulation of the skipping motion

As mentioned in Sec. III A, when the surface potential is stronger than the perpendicular component of the kinetic energy of an outgoing ion, the outgoing ion will be pulled into the solid and be reflected again by the atomic layer, and so on. In other words, an

ion with its ejection angle $\hat{\alpha} < \Delta\alpha$ propagates along the surface with an oscillation similar to skipping motion (the direction R_3 in Fig. 3).

Figure 4 shows the ratio of the number of ions which experience one or more skipping oscillations to that of the incident ions. Here, the neutralization probability is set for two values of C in Eq. (11). The other constants in Eq. (11) are given in a previous paper.⁹ The ratio is a monotonically decreasing function of the angle of incidence. This is mainly due to the facts that the ion reflection rate decreases with the increase of the angle of incidence and that the fraction $\Delta\alpha/\theta_i$ decreases as θ_i increases. Figure 4 also shows the dependence of the ratio N_D/N_i on the direction of the plane of incidence. These ratios for the $\langle 100 \rangle$ plane are twice as large than those for the $\langle 110 \rangle$ plane. This axial dependence of the ratio is

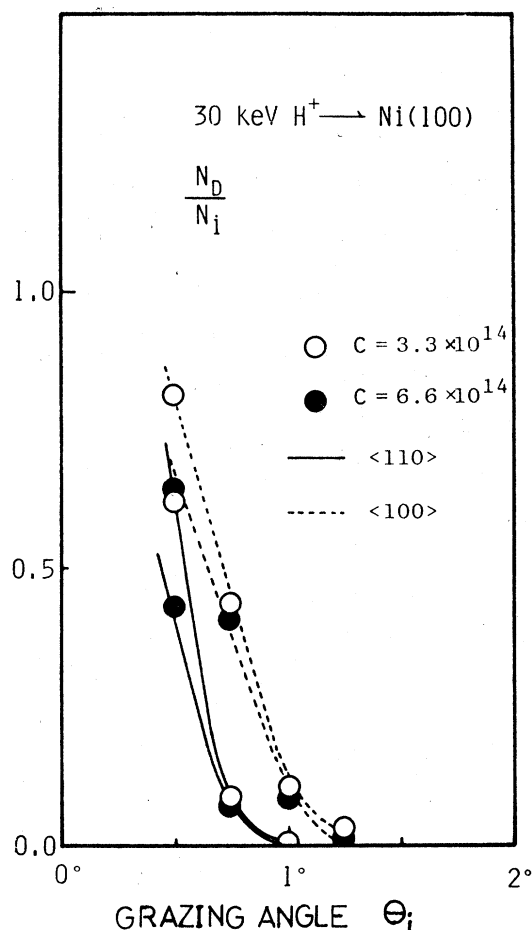


FIG. 4. Dependence of N_D/N_i on the grazing angle θ_i for 30-keV protons going into Ni(100) along the $\langle 110 \rangle$ and $\langle 100 \rangle$ directions. N_D and N_i represent the number of ions which have made one or more skipping oscillations and the number of incident ions, respectively, for two different neutralization parameter C in units of sec^{-1} .

due to the facts that the critical angle for penetration through the $\langle 100 \rangle$ surface along the $\langle 110 \rangle$ rows is smaller than that for penetration along the $\langle 100 \rangle$ atomic rows, and that the ions reflected with small ejection angles from the second layer cannot easily escape from the target since the target surface presents for incoming ions a set of semichannels in the case of the $\langle 110 \rangle$ plane.¹²

It is very interesting to investigate how many times an outgoing ion experiences the skipping oscillation due to the surface force. Figure 5 shows the normalized histogram of the oscillation frequency before the ion escapes from the target, or penetrates deeply into the solid. The ion may escape after it is trapped, because it is neutralized at the surface or scattered by the atoms near the surface. It is notable that even with the present simple model an appreciable amount of ions experience two or more oscillatory motions.

Figure 6 shows the wavelength distributions of the oscillatory motions, where $\lambda_o = L_s/\Delta\alpha$ and λ is the distance between two peaks of the oscillatory motion. It is very interesting that the distribution has a relatively sharp peak under certain conditions.

In Fig. 7 we show ejection angular distributions of ions reflected from the Ni surface compared with or-

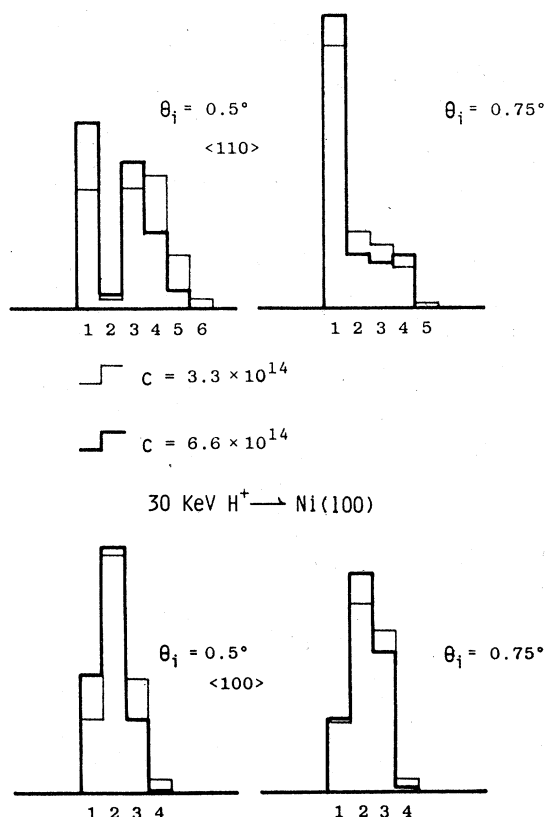


FIG. 5. Normalized histogram of the oscillation frequency of the skipping motions, where the figures on the abscissa are the frequency numbers.

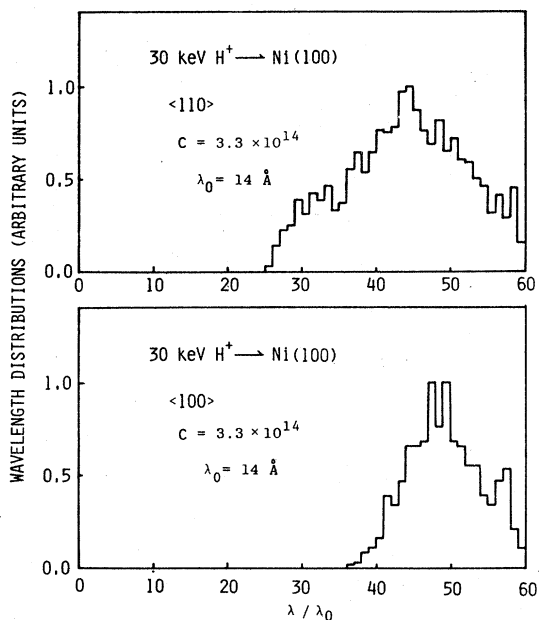


FIG. 6. Wavelength distributions of skipping motions under various incidence conditions.

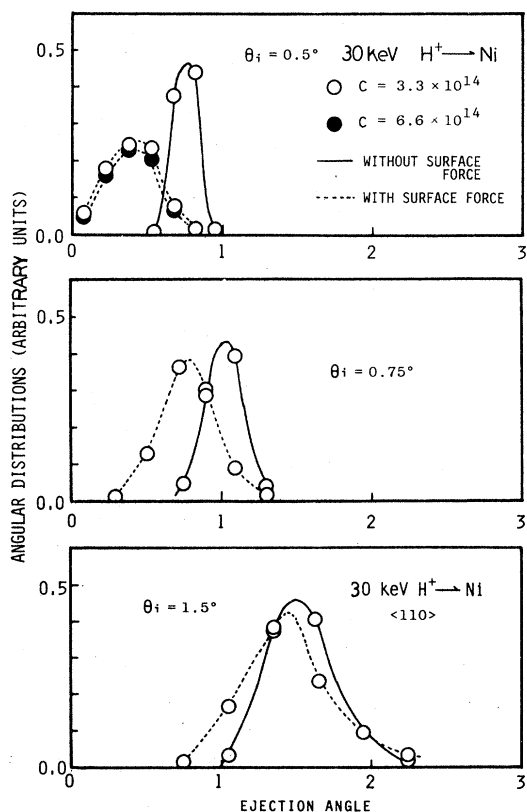


FIG. 7. Ejection-angle dependence of reflected ions at the Ni surface for different grazing angles of 30-keV protons, comparing with the reflected ions without the surface potential.

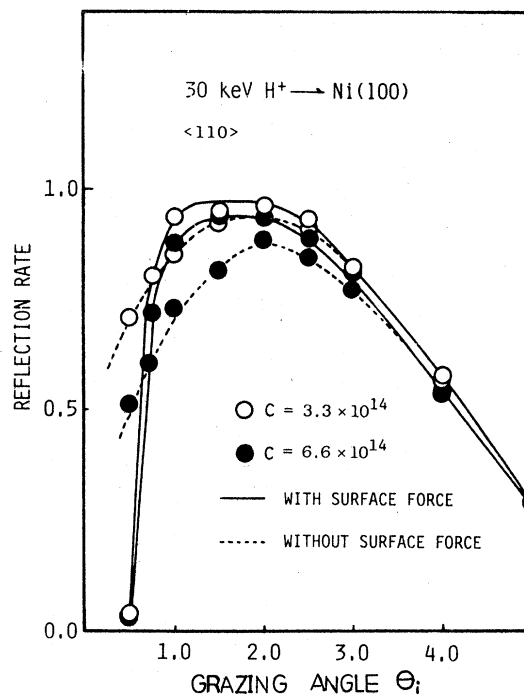


FIG. 8. Grazing-angle dependence of the reflection rate of ions.

inary angular distributions neglecting the surface force. It is worthwhile to note that the peak of the angular distribution is deviated remarkably to a lower ejection angle in the lower-grazing-angle case (see bottom figure, $\theta_i = 0.5^\circ$). We believe that the deviation of the peak will be detected by experiments. The grazing angular dependence of the reflection rate of 30-keV protons is plotted in Fig. 8. We note that

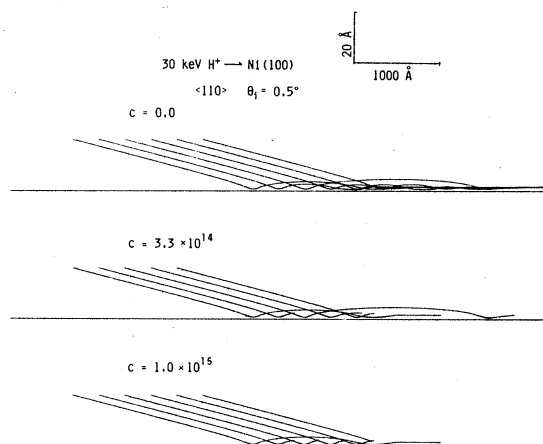


FIG. 9. Examples of 30-keV proton paths near the Ni(100) surface at the grazing angle $\theta_i = 0.5^\circ$ for different neutralization factors. The different scales for "normal to the surface" and "parallel to the surface" are indicated in the figure.

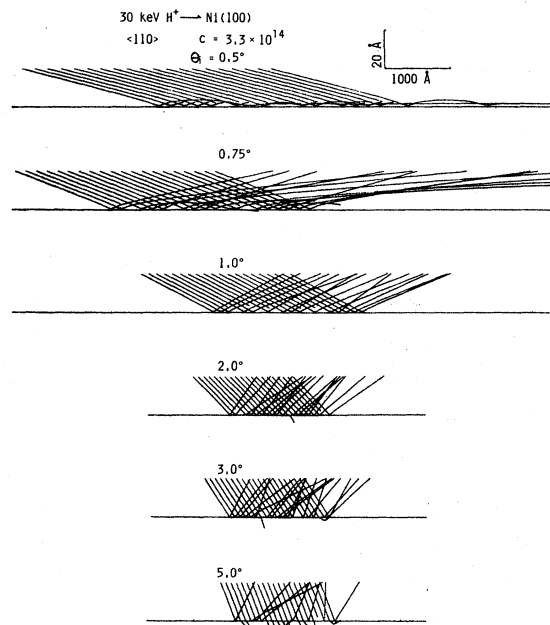


FIG. 10. Examples of 30-keV proton paths for different grazing angles.

the angular distribution decreases abruptly with decreasing grazing angle.

Finally, in Figs. 9 and 10 we show exact path profiles for various neutralization factors and various grazing angles, respectively. Note the different scales for "parallel to the surface" and "normal to the surface". We may recognize that a well-defined skipping

motion takes place in the case of $\theta_i < 0.75^\circ$ and $C < 3.3 \times 10^{14}$.

IV. CONCLUDING REMARKS

We have indicated that the surface potential due to the dynamical polarization of the valence-electron cloud induced by the moving ion has a considerable effect on the surface scattering of the ion itself with grazing angle. When some appropriate conditions are satisfied, the ions cannot escape from the surface due to this potential and are trapped in skipping motions. The computer simulation showed that a large amount of scattered ions goes through with skipping motions and the wavelength distribution of the oscillatory motions has a relatively sharp peak under a certain condition.

The dynamical surface potential will play an important role for secondary-electron emission following bombardment of ions in the metal, since the potential is larger than the work function for electrons near the surface, under some conditions. The Stark effects due to the dynamical surface potential for the He ion or heavier ions near the surface are also interesting phenomena. The study of these topics is in progress by our group.

ACKNOWLEDGMENTS

The authors thank Mr. R. Kawai for his capable assistance in the computation. Thanks are also due to members of our research group in Waseda University for valuable discussions.

¹Atomic Collisions in Solids, edited by F. W. Saris and W. F. van der Weg (North-Holland, Amsterdam, 1976).

²K. Suzuki, M. Kitagawa, and Y. H. Ohtsuki, Phys. Status Solidi B **82**, 643 (1977).

³Y. Yamamura and W. Takeuchi, Radiat. Eff. (to be published).

⁴G. Molière, Z. Naturforsch. **2A**, 133 (1947).

⁵O. B. Firsov, Sov. Phys. JETP **6**, 534 (1958).

⁶E. Everhart, L. K. Verhey, and R. J. Carbone, Phys. Rev. **99**, 1287 (1955).

⁷D. P. Jackson, Surf. Sci. **43**, 431 (1974).

⁸H. D. Hagstrum, Phys. Rev. **96**, 336 (1954).

⁹S. Horiguchi, K. Koyama, and Y. H. Ohtsuki, Phys. Status Solidi B **87**, 757 (1978).

¹⁰O. B. Firsov, Sov. Phys. JETP **9**, 1076 (1959).

¹¹L. C. Northcliffe and R. F. Schilling, Nucl. Data Sect. A **7**, 233 (1970).

¹²V. E. Yurasova, V. I. Schulga, and V. E. Karpuzov, Can. J. Phys. **46**, 759 (1968).